

SOCP Approach for Reducing PAPR System SC-FDMA in Uplink via Tone Reservation

Zid Souad¹ and Bouallegue Ridha²

¹ National Engineering School of Tunis, Tunisia
zidsouad@gmail.com

² SUP'COM, 6'Tel Laboratory, Tunisia
ridha.bouallegue@supcom.rnu.tn

ABSTRACT

The 3rd generation partnership project (3GPP) long term evolution (LTE) standard uses single carrier frequency division multiple access (SC-FDMA) scheme for the uplink transmissions and orthogonal frequency division multiplexing access (OFDMA) in downlink.

In this paper, we point on the Peak-to-Average Power Ratio (PAPR) reduction for the uplink SC-FDMA system. Firstly, the conventional Tone Reservation (TR) is investigated. Then, the approach SOCP (Second Order Cone Programming) is applied for the complex baseband signals of SC-FDMA system with different subcarrier mapping. For the method TR, these subcarriers are located on unused subcarriers of SC-FDMA and we use a raised-cosine pulse. Besides, we prove that the IFDMA can be reduced the PAPR more than the localized FDMA (LFDMA) and distributed FDMA (DFDMA). Finally, this method does not degrade the bit-error-rate (BER) and the data bit rate and no side information (SI) transmission is obligatory.

KEYWORDS

PAPR, SOCP, TR, 3GPP LTE, SC-FDMA, IFDMA, LFDMA &DFDMA

1. INTRODUCTION

SC-FDMA (Single Carrier-Frequency Division Multiple Access) is attracting much attention due to archiving the high speed uplink wireless access. SC-FDMA utilizes single carrier modulation and frequency domain equalization, and has like performance and fundamentally the same overall complexity as those of Orthogonal Frequency Division Multiple Access (OFDMA) system. An important decision for the future mobile radio system is the choice of the multiple access schemes. One possible choice can be the OFDMA like in WiMAX (IEEE 802.16), because of its robustness against frequency selective fading channels and high spectral efficiency. OFDMA is characterized by a high transmit Peak-to-average power ratio (PAPR), and for a given peak-power-limited amplifier this results in a lower mean transmit level. For these reasons, OFDMA is not well suited to the uplink transmission. Single carrier FDMA (SC-FDMA), also known as discrete Fourier transform (DFT) precoded OFDMA, has been proposed in the long term evolution (LTE) standard for the uplink.

In SC-FDMA, there are three methods of assigning the M frequency domain modulation symbols to subcarriers: distributed subcarrier mapping (DFDMA), localized subcarrier mapping (LFDMA), and interleaved subcarrier mapping (IFDMA) [1], [2] a special case of distributed FDMA. In the localized subcarrier mapping mode, the modulation symbols are assigned to M adjacent subcarriers. In the distributed mode, the symbols are equally spaced across the entire channel bandwidth. The distributed and localized mapping of DFT precoded data sequence to OFDM subcarriers is sometimes collectively referred to as DFT-spread OFDM. LFDMA incurs higher PAPR compared to IFDMA [3], [4]. Though IFDMA is more desirable than LFDMA in terms of PAPR power efficiency, LFDMA is clearly superior in terms of throughput when

channel dependent scheduling is utilized. In [5] the statistical PAPR characteristics are investigated for OFDM signals. Different techniques for PAPR reduction in OFDM signals are summarized in [5]. Various researches are still going on to find the impact of diverse parameters on PAPR in SC-FDMA.

To further reduce the PAPR in SC-FDMA, Tone Reservation (TR) techniques used to reduce the PAPR in SC-FDMA can be a potential choice. In this paper, we will propose a modeling in the form of Second Order Cone Programming (SOCP) with additional constraints, in particular, with the constraint of an additional power lower than a certain threshold acceptable for the application.

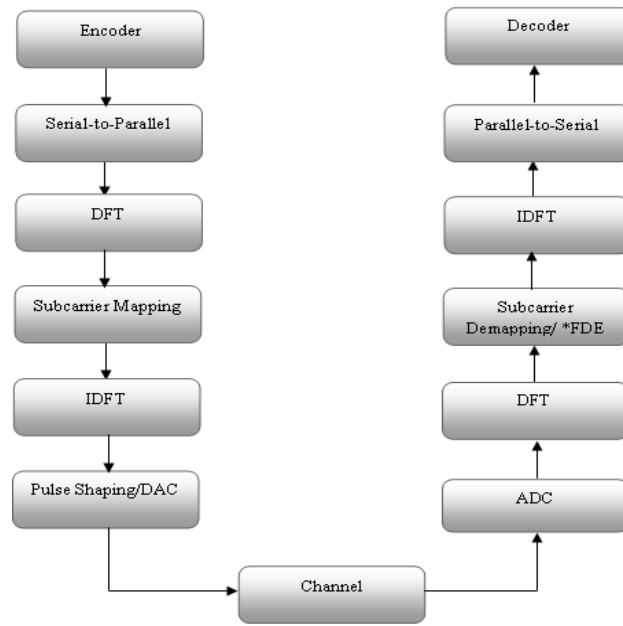
Besides, we include the incorporations of constraints on the relative mean power. In this approach we suggest to allocate a set of tones in each band of the system SC-FDMA. Our objective is to improve the reduction of the PAPR without any degradation of the BER and data bit rate degradation and without sending any SI. To do so, we will use the unused carriers to generate the corrective signal. The receiver does not get these subcarriers into account and thus needs no modification [18]. It has been applied in a single input single output (SISO) context with a SOCP optimization algorithm with the method Tone Reservation (TR).

The rest of this paper is organized as follows. In Section 2, overview of SC-FDMA system is reviewed. Section 3 introduces the subcarrier mapping for SC-FDMA. Then an improved minimizing PAPR via optimization technique was proposed in Section 4. The simulation results and performance analysis are shown in Section 5. Finally, conclusions are given in Section 6.

2. OVERVIEW OF SC-FDMA SYSTEM

Single-carrier frequency division multiple access (SC-FDMA) is a modulation format standardized for the transmission in the uplink of LTE. Also referred to as discrete Fourier transform (DFT) precoded orthogonal frequency division multiple access (OFDMA), it combines the advantages of OFDMA and single-carrier transmission [6], i.e., high data rates and simple frequency domain equalization are obtained along with lower peak-to-average power ratio compared to OFDMA.

A block diagram of a SC-FDMA system is shown in Figure 1. SC-FDMA can be regarded as discrete Fourier transform (DFT)-spread OFDMA, where time domain data symbols are transformed to frequency domain by DFT before going through OFDMA modulation. The orthogonality of the users stems from the fact that each user occupies different subcarriers in the frequency domain, similar to the case of OFDMA. Because the overall transmit signal is a single carrier signal, PAPR is inherently low compared to the case of OFDMA which produces a multicarrier signal [19].



*FDE :Frequency Domain Equalization

Figure 1. A block diagram of an SC-FDMA system.

Figure 2 details the generation of SC-FDMA transmit symbols. There are M subcarriers, among which $N (< M)$ subcarriers are occupied by the input data. In the time domain, the input data symbol has symbol duration of T seconds and the symbol duration is compressed to $\hat{T} = \left(\frac{N}{M}\right) \cdot T$ after going through SC-FDMA modulation.

There are two methods to choose the subcarriers for transmission as shown in Figure 3. In the distributed subcarrier mapping mode, DFT outputs of the input data are allocated over the entire bandwidth with zeros occupying in unused subcarriers, whereas consecutive subcarriers are occupied by the DFT outputs of the input data in the localized subcarrier mapping mode. We will refer to the localized subcarrier mapping mode of SC-FDMA as localized FDMA (LFDMA).

The case of $M = Q \cdot N$ for the distributed mode with equidistance between occupied subcarriers is called Interleaved FDMA (IFDMA). An example of SC-FDMA transmit symbols in the frequency domain for $N = 4$, $Q = 4$ and $M = 16$ is illustrated in Figure 4. After subcarrier mapping, the frequency data is transformed back to the time domain by applying inverse DFT (IDFT).

Figure 1 shows the schematic diagram of the SC-FDMA system. At the transmitter, the encoded data are transformed to a multilevel sequence of complex numbers in one of several possible modulation formats. The resulting modulated symbols are grouped into blocks, each containing N symbols and the discrete Fourier transform (DFT) is performed. Then, the subcarriers are mapped in the frequency domain. After that, the inverse discrete Fourier transform (IDFT) is performed and a cyclic prefix (CP) is added to the resulting signal. Finally, the resulting signal is transmitted through the wireless channel.

The signal after the DFT can be expressed as follows

$$X_{q,k} = \sum_{n=0}^{N-1} x_{q,n} e^{-\left(\frac{j2\pi}{N}\right)nk} \quad (1)$$

where $\{x_{q,n}: n = 0, \dots, N - 1\}$ represents the modulated data symbols of user q . N is the *DFT* length. After the *IDFT*, the signal can be expressed as follows

$$\bar{x}_{q,m} = \frac{1}{M} \sum_{l=0}^{M-1} \bar{X}_{q,l} e^{\left(\frac{j2\pi}{M}\right)ml} \quad (2)$$

where $\{\bar{X}_{q,l}: l = 0, \dots, M - 1\}$ represents the frequency domain samples after subcarrier mapping. M is the IDFT length (subcarrier number) ($M > N$). $\{\bar{x}_{q,m}: m = 0, \dots, M - 1\}$ represents the time symbols after the IDFT.

The complex pass band transmit signal of SC-FDMA $x_q(t)$ for a block of data is represented as

$$x_q(t) = e^{jw_c t} \sum_{m=0}^{M-1} \bar{x}_{q,m} r(t - m\tilde{T}) \quad (3)$$

where w_c is the carrier frequency of the system and $r(t)$ is the baseband pulse. In our research, we use a raised-cosine pulse, which is a widely used pulse shape in wireless communications, defined as follows in the time domain [7]

$$r(t) = \text{sinc}\left(\pi \frac{t}{\tilde{T}}\right) \frac{\cos\left(\frac{\alpha\pi t}{\tilde{T}}\right)}{1 - \frac{4\alpha^2 t^2}{\tilde{T}^2}} \quad (4)$$

where α is the roll off factor which ranges between 0 and 1.

Frequency domain pulse shaping is performed using a raised cosine filter. For QPSK modulation the effect of pulse shaping is shown for different values of raised cosine roll off factor α .

The power of the raised cosine filter is normalized to unity for all values of α . Since the raised cosine filter gives a smaller output peak power level with increasing α , we note that the PAPR reduces as α increases.

The length of the CP must be greater than the maximum excess delay of the channel to accommodate the interblock interference (IBI). The baseband channel response can, then, be expressed as follows [8], [9]

The multi-carrier signal of user q , namely $x_q = \{\bar{x}_{m,q}\}$, is the sum of many independent signals modulated on subcarriers. PAPR was widely used to evaluate envelope fluctuations of signals. PAPR of SC-FDMA signals without pulse shaping with symbol rate sampling can be expressed in [10]. The corresponding discrete-time PAPR for user q in an SC-FDMA uplink system is defined as

$$PAPR = \frac{\max_{m=0,1,\dots,M-1} |\bar{x}_{m,q}|^2}{\frac{1}{M} \sum_{m=0}^{M-1} |\bar{x}_{m,q}|^2} \quad (5)$$

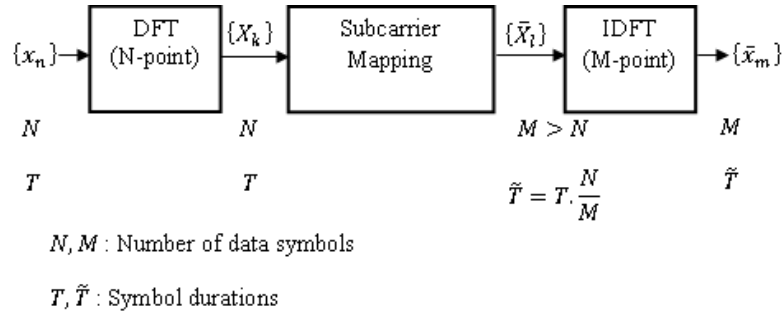


Figure 2. Generation of SC-FDMA transmit symbols. There are M total number of carriers, among which $N (< M)$ subcarriers are occupied by the input data.

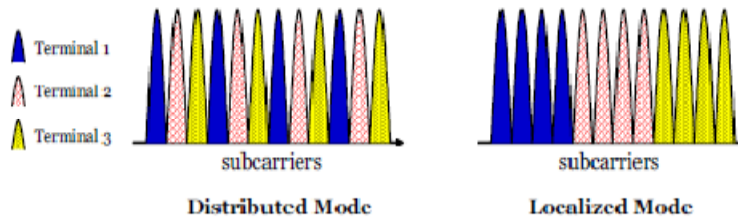


Figure 3. Subcarrier allocation methods for multiple users ($Q=3$ users, $M=12$ subcarriers, and $N=4$ subcarriers allocated per user)

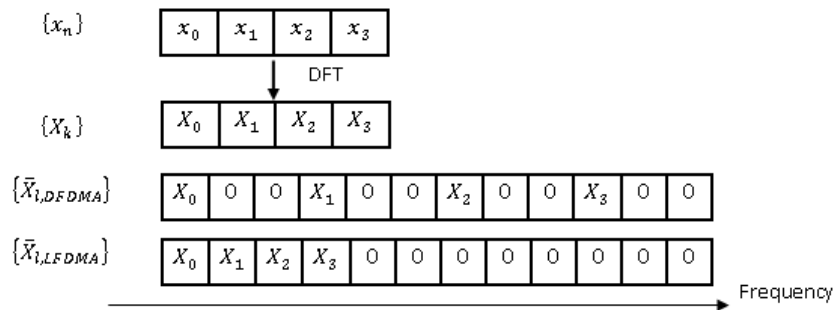


Figure 4. An example of SC-FDMA transmit symbols in the frequency domain for $N = 4$, $Q = 4$ and $M = 16$.

$\{\bar{X}_{L,DFDMA}\}$ denotes transmit symbols for distributed subcarrier mapping mode and $\{\bar{X}_{L,LFDMA}\}$ denotes transmit symbols for localized subcarrier mapping mode.

3. SUBCARRIER MAPPING

In this section, we are two methods to choose the subcarriers mapping for transmission; *distributed* subcarrier mapping and *localized* subcarrier mapping. In the distributed subcarrier mapping mode, DFT outputs of the input data are allocated over the entire bandwidth with zeros

occupying the unused subcarriers, whereas consecutive subcarriers are occupied by the DFT outputs of the input data in the localized subcarrier mapping mode. We will refer to the localized subcarrier mapping mode of SC-FDMA as localized FDMA (LFDMA) and distributed subcarrier mapping mode of SC-FDMA as distributed FDMA (DFDMA). The case of $M = Q \times N$ for the distributed mode with equidistance between occupied subcarriers is called Interleaved FDMA (IFDMA) [11], [12]. IFDMA is a special case of SC-FDMA and it is very efficient in that the transmitter can modulate the signal strictly in the time domain without the use of DFT and IDFT. An example of SC-FDMA subcarrier mappings in the frequency domain for $N = 4$, $Q = 3$ and $M = 12$ is illustrated in Figure 3. Depending on the subcarrier mapping method, the SCFDMA modulated symbols in the time domain differ [13].

For IFDMA, the modulated time symbols are simply a repetition of the original input symbols with a scaling factor of $1/Q$ and some phase rotation. DFDMA and LFDMA have the same time symbol structure; they have exact copies of input time symbols with a scaling factor of $1/Q$ in the N -multiple sample positions and in-between values are sum of all the time input symbols in the input block with different complex weighting. Because of this, we can expect to see more fluctuation and higher peak in amplitude for DFDMA and LFDMA.

One strategy for PAPR reduction is to search an additive corrective signal c_q in order to have $PAPR(x_q + c_q) < PAPR(x_q)$. This approach belongs to the additive signal methods for PAPR reduction. One way to find c_q is to use optimization approaches, what is detailed in the next section.

In this paper, the PAPR (minimizing) is evaluated in terms of its Complementary Cumulative Distribution Density Function (CCDF), that is, the probability that the PAPR exceeds a given threshold.

4. MINIMIZING PAPR VIA OPTIMIZATION TECHNIQUE

The approach used in this paper is to add an artificial signal to unused carriers. The signal addition is achieved in frequency domain. Thus, the PAPR of the resulting signal ($x_q + c_q$) is given by:

$$PAPR\{x_q + c_q\} = \frac{\max_{0 \leq m \leq M-1} \{|\bar{x}_{m,q} + \bar{c}_{m,q}|^2\}}{E\{|\bar{x}_{m,q}|^2\}} \quad (6)$$

In this section, we introduce a PAPR reduction scheme for mobile users sharing an SC-FDMA uplink. In the previous section, for each user in the SC-FDMA uplink, a small set of subcarriers are used to transmit data. In this method tone reservation for SC-FDMA we propose to allocate a set of tones in each of the B_q subbands for PAPR reduction. In contrast of [17] we propose to allocate exactly one tone in each of the B_q subbands. All users and the base station (BS) know the positions of the reserved tones. The set of tones reserved, no data is transmitted and the reserved tones do not interfere with data transmission.

Each user can design its compensating signal C_q without knowledge of other users' compensating signals. There are two possibilities of positioning of tone reserved as in the middle or in the highest frequency of each subband. The data-rate loss for user q of N_q/N , where N_q is the number of reserved tones of user q . Since N is small when compared to M .

The objective is to search C_q to reduce the PAPR of original X_q , in order to simplify this problem, uses a Quadrature Constraint Quadrature Programming(QCQP) to find the corrective

signal C_q for each user. Each user is characterized by the signal compensation C_q and each user solves the following optimization problem:

$$\hat{C}_q = \arg \min_{C_q} \|x_q + Q_R C_q\|_\infty, \quad q = 1, \dots, Q \quad (7)$$

In (10), R denotes the index set of the reserved tones, $C_q \in \mathbb{C}^{N_q \times 1}$ is the decision variable, and Q_R is submatrix of Q , obtained by the selecting the columns according to R . The compensating signal is formed by the elements of \hat{C}_q via:

$$c_{m,q} = \frac{1}{M} \sum_{k \in R} \hat{C}_{k,q} e^{j2\pi km/M}, \quad m = 1, \dots, M - 1 \quad (8)$$

Where $\hat{C}_{k,q}$ is the k th element of \hat{C}_q , we can note $\psi_{i_r} = e^{2\pi i_r m/M}$ and $R = \{i_0, i_1, \dots, i_{N_q}\}$.

The corrective signal we can write by this expression:

$$\begin{aligned} c_q &= \frac{1}{M} \sum_{r=0}^{N_q} C_{i_r,q} e^{j\psi_{i_r}} = \frac{1}{M} \sum_{r=0}^{N_q} [(C_{i_r,q}^{re} + jC_{i_r,q}^{im})(\cos(\psi_{i_r}) + jsin(\psi_{i_r}))] \\ &= \frac{1}{M} \sum_{r=0}^{N_q} [(C_{i_r,q}^{re} \cos(\psi_{i_r}) - C_{i_r,q}^{im} \sin(\psi_{i_r}))] \\ &\quad + j \frac{1}{M} \sum_{r=0}^{N_q} [(C_{i_r,q}^{re} \sin(\psi_{i_r}) + C_{i_r,q}^{im} \cos(\psi_{i_r}))] \quad (9) \end{aligned}$$

Where $C_{i_r,q}^{re} = \Re(C_{i_r,q})$ and $C_{i_r,q}^{im} = \Im(C_{i_r,q})$ and N_q denote the number of tone reservation. So, the PAPR for OFDMA system minimization problem can be written as:

$$\min_{c_q} \|x_q + c_q\|_\infty = \min_{C_q} \|x_q + Q_R C_q\|_\infty = \min_{C_q} \max_m |x_{m,q} + Q_R^{(m)} C_q| \quad (10)$$

where $C_q = [C_{i_0,q}, C_{i_1,q}, \dots, C_{i_{N_q-1},q}]$, is the submatrix of Q constructed by choosing its columns with the indices of R , Q denotes the inverse discrete Fourier transform of size $(M \times M)$ and $Q_R^{(m)}$ is the m th row of Q_R .

The above convex optimization problem is also equivalent to:

$$\begin{aligned} & \min t \\ & \text{subject to : } |x_{m,q} + Q_R^{(m)} C_q| \leq t, 0 \leq m \leq M - 1 \quad (11) \end{aligned}$$

SOCP is a convex optimization problem class that minimizes a linear function over the intersection of an affine set and the product of second-order (quadratic) cones [14], [18]. Special Issue on Linear Algebra in Control Signals and Image Processing. A general second-order cone program could take the form of

$$\begin{aligned} & \min F^T Y \\ & \text{subject to : } \|A_p Y + H_p\| \leq E_p^T Y + g_p \\ & p = 0, \dots, P - 1 \quad (12) \end{aligned}$$

where $Y \in \mathbb{R}^m$ is the optimization variable while $F \in \mathbb{R}^m$, $A_p \in \mathbb{R}^{(m_p-1) \times m}$, $H_p \in \mathbb{R}^{(m_p-1)}$, $E_p \in \mathbb{R}^m$ et $g_p \in \mathbb{R}$ are the problem parameters. $\|\cdot\|$ denotes the Euclidean norm.

Due to SOCP characterization, it is easy to see the above convex optimization problem given by equation (11) can be reformulated as a SOCP with:

$$|A_m Y + H_m| \leq E_m^T Y + g_m \quad (13)$$

where:

$$A_m = \begin{bmatrix} \cos_{\psi_{i_0}}(m) - \sin_{\psi_{i_0}}(m) \cdots \cos_{\psi_{i_{N_q-1}}}(m) - \sin_{\psi_{i_{N_q-1}}}(m) & 0 \\ \sin_{\psi_{i_0}}(m) \cos_{\psi_{i_0}}(m) \cdots \sin_{\psi_{i_{N_q-1}}}(m) \cos_{\psi_{i_{N_q-1}}}(m) & 0 \end{bmatrix} \in \mathbb{R}^{2 \times (2N_q+1)} \quad (14)$$

$$Y = \begin{bmatrix} C_{i_0,q}^{re} \\ C_{i_0,q}^{im} \\ \vdots \\ C_{i_{N_q-1},q}^{re} \\ C_{i_{N_q-1},q}^{im} \\ t \end{bmatrix} \in \mathbb{R}^{(2N_q+1) \times 1} \quad (15)$$

$$H_m = \begin{bmatrix} \Re(x_{m,q}) \\ \Im(x_{m,q}) \end{bmatrix} \in \mathbb{R}^{2 \times 1} \quad (16)$$

$$E_m^T = [0 \ 0 \ \cdots \ 0 \ 1] \in \mathbb{R}^{2N_q+1} \quad (17)$$

$$g_m = 0 \in \mathbb{R} \quad (18)$$

When we pose :

$$F_m^T = [0 \ 0 \ \cdots \ 0 \ 1] \in \mathbb{R}^{2N_q+1} \quad (19)$$

Starting from the preceding relations (14) to (19) we can deduce that our problem of reduction of the PAPR modeled in the form of convex problem of optimization given by relation (11) is well a problem SOCP given by formula (12).

Many free software solvers exist to solve the convex optimization problem among which SeDuMi, YALMIP, and CVX [15]. All this software are very easy to use. For our simulation we have chosen YALMIP. However, adding a signal c_q to x_q to reduce the PAPR increases the transmit power. The relative increase mean power ΔE , due to PAPR reduction is defined as [16]

$$\Delta E = 10 \log_{10} \frac{E(\|x_q + c_q\|^2)}{E(\|x_q\|^2)} \quad (20)$$

The parameter must be as small as possible in order to be compatible with current power amplifiers. Indeed, it is easy to understand that if one increases indefinitely the average power of the signal $x_q + c_q$ one would have obviously $PAPR = 0dB$ but a signal which cannot be transmitted. Thus, the relative mean power must be upper bounded and can be written as:

$$\Delta E \leq \gamma_{dB} \quad (21)$$

That is

$$E\left(\|x_q + c_q\|^2\right) \leq \lambda E\left(\|x_q\|^2\right) \quad (22)$$

Where $\lambda = 10^{\frac{\gamma}{10}}$ γ is a constant closely related to the characteristic of the amplifier.

The above condition can be added as a constraint in the optimization problem. The optimization problem then becomes

$$\begin{aligned} & \min t \\ & \text{subject to : } |x_{m,q} + Q_R^{(m)} C_q| \leq t, 0 \leq m \leq M - 1 \\ & \|x_q + Q_R C_q\| \leq \sqrt{\lambda K} \quad (23) \end{aligned}$$

Where $K = NE\left(|x_q|^2\right)$

5. SIMULATION RESULTS

In order to evaluate the performance of the proposed method, PAPR CCDF curves of an SC-FDMA signal is presented. To solve the convex optimization problem, a free software known as YALMIP is used. In our simulations, the bandwidth of 5MHz is divided into $M = 256$ subcarriers and QPSK constellation. The system can support $Q = 8$ users to communicate with the BS simultaneously. Each user occupies $N = 32$ successive subcarriers. For each user's subband, only a set of subcarriers $N_q = 6$ is used as the reserved tone for PAPR reduction. In the simulation, we focus on the first user as the desired user. To evaluate the PAPR reduction performance, we concentrate on the complementary cumulative distribution function of the user's PAPR. Figure 5 compares the PAPR CCDF of the original signal with that of reduced PAPR signal without any constraint for the system SC-FDMA. This PAPR reduction gain is obtained to the detriment of a relative mean transmitted power increase ΔE .

Figure 6 plots the CCDF of the optimized signal vs γ for the system SC-FDMA. As we can see, the PAPR decreases as γ increases. We have concluded that the IFDMA is better than the LFDMA and DFDMA systems in terms of CCDF PAPR.

Figure 7 shows the impact of rolloff factor α on the PAPR when using raised cosine pulse shaping, where this impact is more obvious in DFDMA. As the rolloff factor increases from 0 to 1, PAPR reduces significantly for DFDMA.

Figure 8 shows the impact of rolloff factor α on the PAPR when using raised cosine pulse shaping, where this impact is more obvious in IFDMA. As the rolloff factor increases from 0.1 to 0.9, PAPR reduces significantly for IFDMA.

6. CONCLUSION

In this paper, we have proposed a new PAPR reduction for the system SC-FDMA, This approach is based on SOCP and provides important PAPR reduction gains not including transmitting any side information and without degrading BER and data rate at the same time. To do so, we have used the unused tones of the standards to generate the corrective signal in each user. We have shown that the performances given by our approach, the PAPR can be reduced about 3dB at 10^{-3} probability level. We have concluded that the IFDMA is better than the LFDMA and DFMA systems in terms of CCDF PAPR. To avoid an increase of the relative

mean power, we have added an additional constraint and the results still show significant gains on the CCDF of the PAPR.

An additional obvious fact is that pulse shaping increases PAPR and that rolloff factor in the case of raised-cosine pulse shaping has a significant impact on PAPR of DFDMA. A pulse shaping filter should be considered carefully in order to reduce the PAPR not including corrupting the system performance.

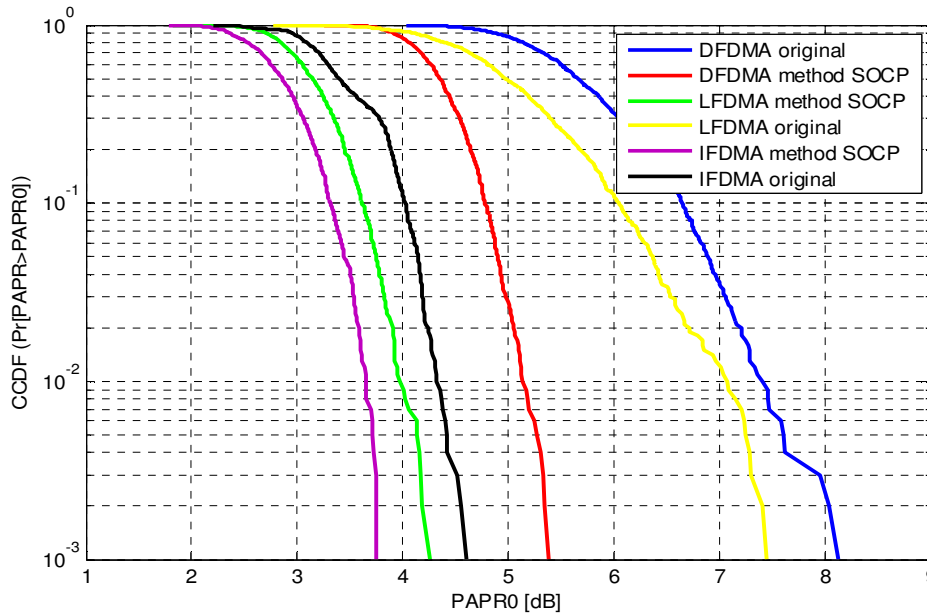


Figure5. CCDF performance of method using SOCP with unused tones as reserved tones and roll off factor $\alpha=0.5$ for the LFDMA, DFDMA and IFDMA

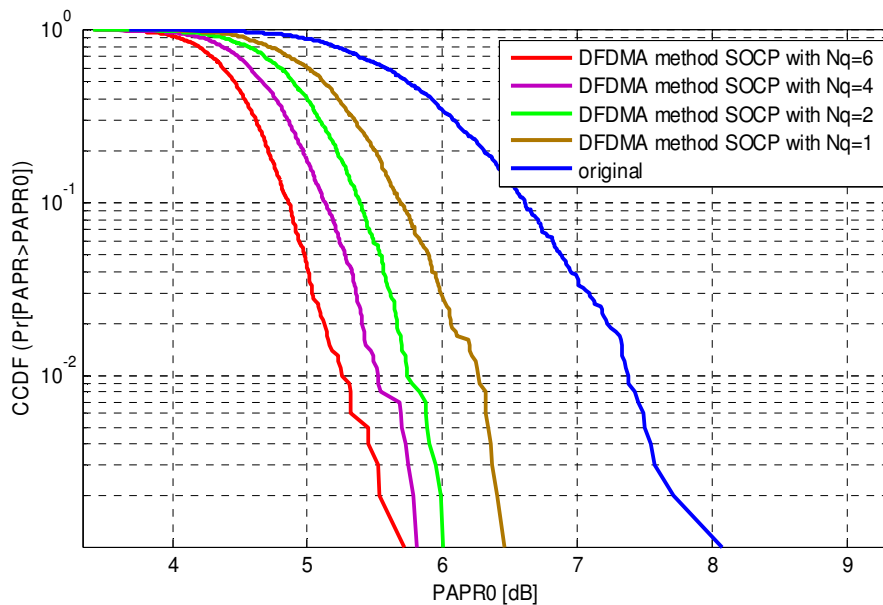


Figure6. CCDF performance of method using SOCP with unused tones as reserved tones increases from 1 to 6 and roll off factor $\alpha=0.2$ for the DFDMA

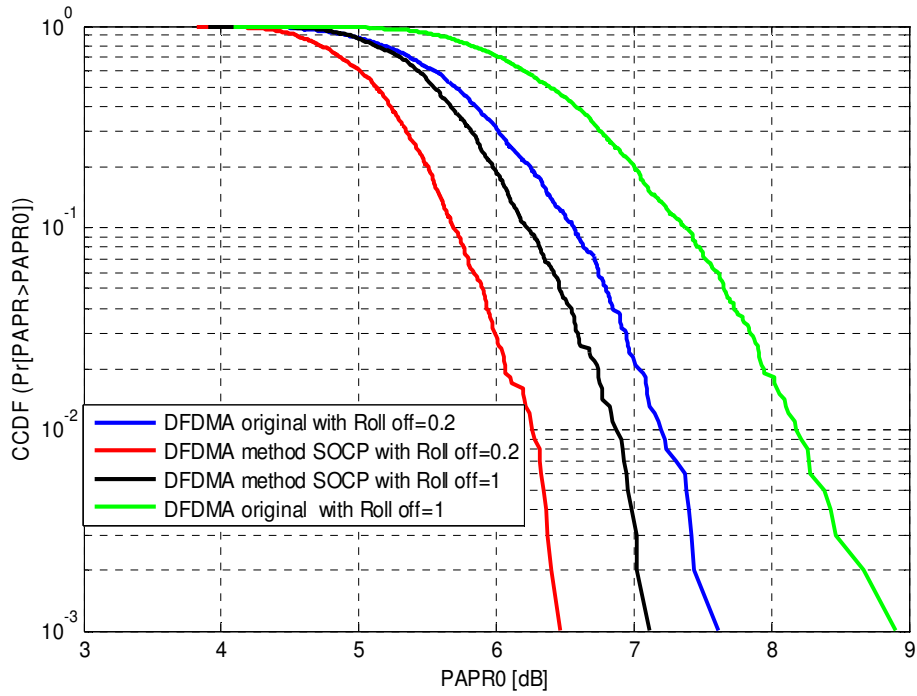


Figure7. CCDF performance of method using SOCP with one unused tone as reserved tones and roll off factor α increases from 0.2 to 1 for the DFDMA

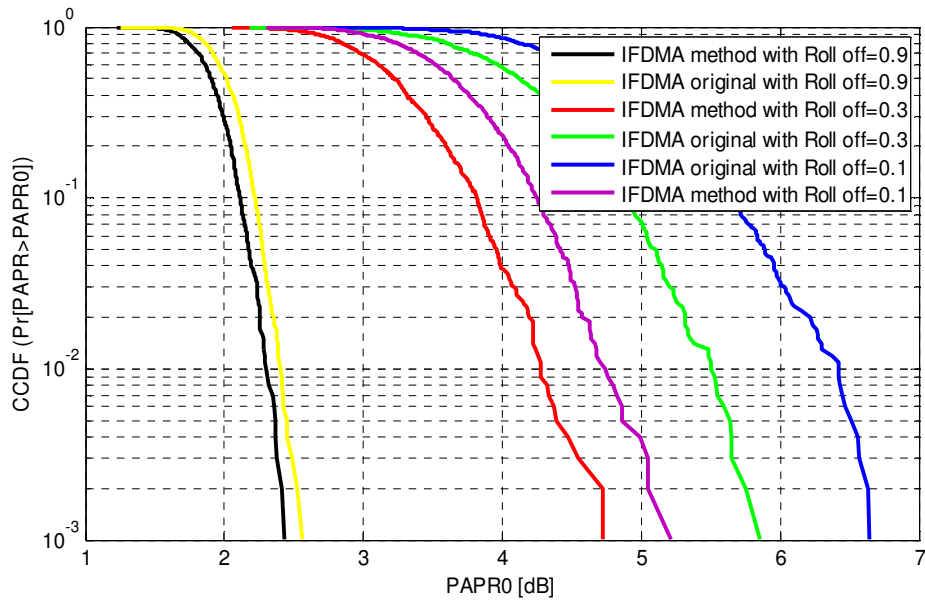


Figure8. CCDF performance of method using SOCP with 6 unused tone as reserved tones and roll off factor α increases from 0.1 to 0.9 for the IFDMA

REFERENCES

- [1] Hyung G. Myung, David J. Goodman, (2008) "Single Carrier FDMA": A New Air Interface for Long Term Evolution. John Wiley & Sons, Ltd.
- [2] S. Sesia, I. toufik, and M. Baker, (2009) "LTE-The UMTS Long Term Evolution From Theory to Practice". John Wiley & Sons, Ltd.
- [3] 3GPP R1-050475. (2005) "PAPR comparison of uplink MA schemes", 3GPP. TSG RAN WG1 Meeting #41, Athens, Greece.
- [4] H. G. Myung, J. Lim, and D. J. Goodman, (2006)"Single carrier FDMA for uplink wireless transmission", *IEEE Vehicular Technology Magazine*, vol. 1, no. 3, pp. 30-38.
- [5] T. Jiang and Y. Wu, (2008) "An Overview: Peak-to-Average Power Ratio Reduction Techniques for OFDM Signals," *IEEE Trans. Broadcasting*, vol. 54.
- [6] H. G. Myung, (2007) "Single Carrier Orthogonal Multiple Access Technique," Ph.D. dissertation, Polytechnic University.
- [7] T. S. Rappaport, (2002) *Wireless Communications: Principles and Practice*, Second Edition. Prentice Hall.
- [8] AL-KAMALI F.S., DESSOUKY M.I., SALLAM B.M., EL-SAMIE F.E. (2009) "Performance evaluation of cyclic prefix CDMA systems with frequency domain interference cancellation", *Digital Signal Process.*, vol. 19, (1), pp. 2-13
- [9] ADACHI F., GARGE D., TAKAOKA S., TAKEDA K. (2005) "Broadband CDMA techniques", *IEEE Wirel. Commun.*, vol. 12, (2), pp. 8-18
- [10] Myung H. G., Junsung Lim, and Goodman D. J., (2006) "Peak-to-average Power Ratio of Single Carrier FDMA Signals with Pulse Shaping", *IEEE International Symposium on Personal, Indoor and Mobile Radio Communications*.
- [11] U. Sorger, I. De Broeck, and M. Schnell, (1998) "Interleaved FDMA - A New Spread-Spectrum Multiple-Access Scheme," *Proc. IEEE ICC '98*, Atlanta, GA, pp. 1013-1017,
- [12] M. Schnell and I. De Broeck, (1998) "Application of IFDMA to Mobile Radio Transmission," *Proc. IEEE 1998 International Conference on Universal Personal Communications (ICUPC '98)*, Florence, Italy, pp. 1267-1272.
- [13] H. G. Myung, (2007) "Single Carrier Orthogonal Multiple Access Technique for Broadband Wireless Communications," Ph.D. Dissertation, Polytechnic University, Brooklyn, NY.
- [14] M. Lobo, L. Vandenberghe, S. Boyd and H. Lebret, (1998) "Applications of Second Order Cone Programming", *Linear Algebra and its Applications*, 284:193-228.
- [15] M. Grant, S. Boyd, and Yinyu Ye, "CVX -Matlab Software for Disciplined Convex Programming", <http://www.stanford.edu/boyd/cvx/>.
- [16] Jose Tellado-Mourelo, (1999)"Peak-to-Average Power Ratio Reduction for Multicarrier Modulation", PhD thesis, Stanford University.
- [17] Meng Wang, Daniel E. Quevedo, Graham C. Goodwin and Brian S. Krongold, (2007) "OFDMA Uplink PAR Reduction via Tone Reservation", *Proc. IEEE GLOBECOM 2007*, pp. 3802-3806.
- [18] Basel RIHAWI, Yves LOUET, (2008) "PAPR reduction scheme with SOCP for MIMO-OFDM systems", *International Journal of Communications, Network and Systems Sciences (IJCNS)*, pp. 29-35.
- [19] H. G. Myung, J. Lim, and D. J. Goodman, (2006) "Peak-to average Power Ratio of Single Carrier FDMA Signals with Pulse Shaping", *Proc. IEEE International Symposium on Personal, Indoor and Mobile Radio Communications (PIMRC) 2006*.